

# Microphysics and convection in the ‘grey zone’

Luc Gerard

*RMIB, 3 Av. Circulaire,  
B1180 Brussels  
luc.gerard@meteo.be*

## ABSTRACT

We assess the behaviour of a limited area NWP model with different handlings of deep convection when varying the grid-box length from 8 to 1km.

## 1 Introduction

When the grid-box length is close to the dimensions of deep-convection (DC) cells or systems, these are badly handled by the kind of DC-parametrization commonly used in coarser resolution models. On the other hand, trying to treat them explicitly (with no parametrization) is neither satisfactory. More specific approaches are required to run at these ‘grey-zone resolutions’. Here we compare the behaviour of different approaches in an academic case and in a real case.

Four ways to handle deep convection are tried: no specific parametrization (*nocp*), the Bougeault diagnostic scheme (*dia*), the 3MT package (*3MT*) (Gerard *et al.* 2009) and our new *complementary subgrid updraught* approach (*CSU*).

## 2 Academic experiment and schemes features

The academic setup is inspired from Weisman and Klemp (1982) and uses their same vertical profile of temperature, moisture and wind over the entire cyclic domain. At the centre of the domain (and at a height equal to its radius) we add a potential-temperature perturbation with a vertical radius of 1400m, a horizontal radius of 3km, that we assume to be resolved by a 1km grid-length mesh. The perturbation is maximum (2K) at its centre, decreasing to zero at its border. The model has 85 isobar vertical levels and is run with a non-hydrostatic dynamics; the radiation scheme is switched off.

The *nocp* 1-km experiment is taken as a reference. The *nocp* setup cannot produce precipitation at 8km resolution, and gives a too narrow and too intense pattern at 4km (Fig. 1, left column). The *dia* experiment (Fig. 2, left column) gives a (too weak) signal at 8km, but a much too wide and intense area at 4 and 2km, with an important contribution of the subgrid. The wind and the resolved circulation are further affected by the inadequate response of the DC parametrization.

The 3MT approach was developed to produce a smoother response down to resolutions around 4km. It prevents that the subgrid (deep convection) and the resolved condensation parametrizations both feed on the same available moisture, by using a sequential organisation of the parametrizations. The deep convection scheme affects the resolved model variables through condensation and transport fluxes, and its condensation fluxes are combined with the ones from the resolved scheme, before being passed to the microphysical scheme. In addition, evolutive aspects are included by using prognostic variables for

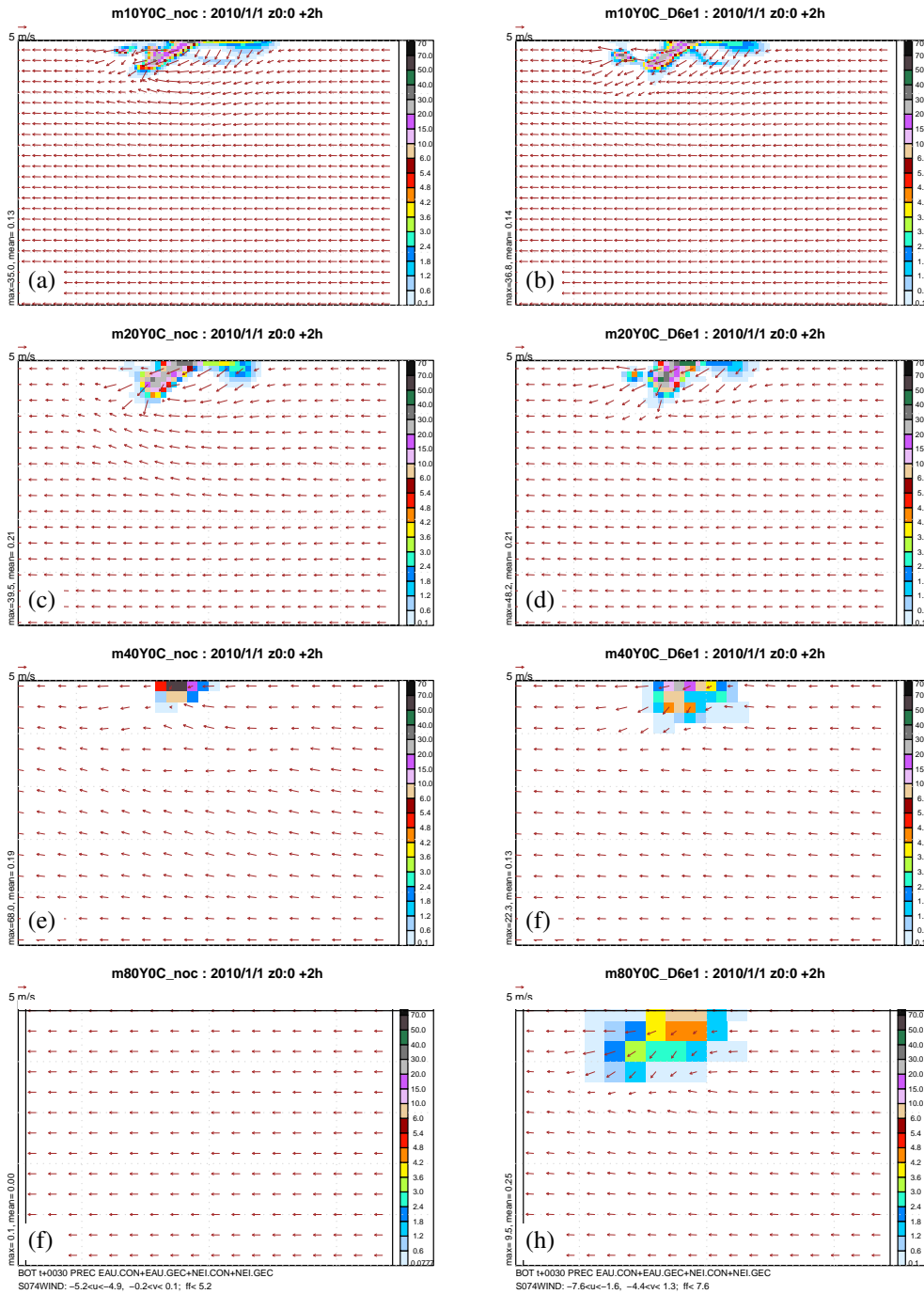


Figure 1: 2-hour accumulated parametrization, over the lower half of the symmetric domain. Left: ‘nocp’; right: new ‘CSU’ scheme. (a,b):  $\Delta x=1\text{km}$ ; (c,d):  $2\text{km}$ ; (e,f):  $4\text{km}$ ; (g,h):  $8\text{km}$ .

the updraught vertical velocity (non-hydrostatic vertical motion equation) and the updraught mesh fraction (prognostic closure). The microphysics considers subgrid cloud and precipitation fraction overlaps depending on the relative subgrid and resolved shares of the condensation. Finally, a memory of the convective cloud fraction (updraught + detrainment fraction) is also used from one time step to the next, to prevent a re-evaporation of not yet precipitated convective condensate that could occur if this was assumed to be distributed over the entire grid box. The 3MT scheme as used in the Alaro-0 model has brought a significant improvement in the operational forecast of cloud and precipitation; however, while allowing a relatively smooth evolution, the subgrid share does not diminish with decreasing grid-box

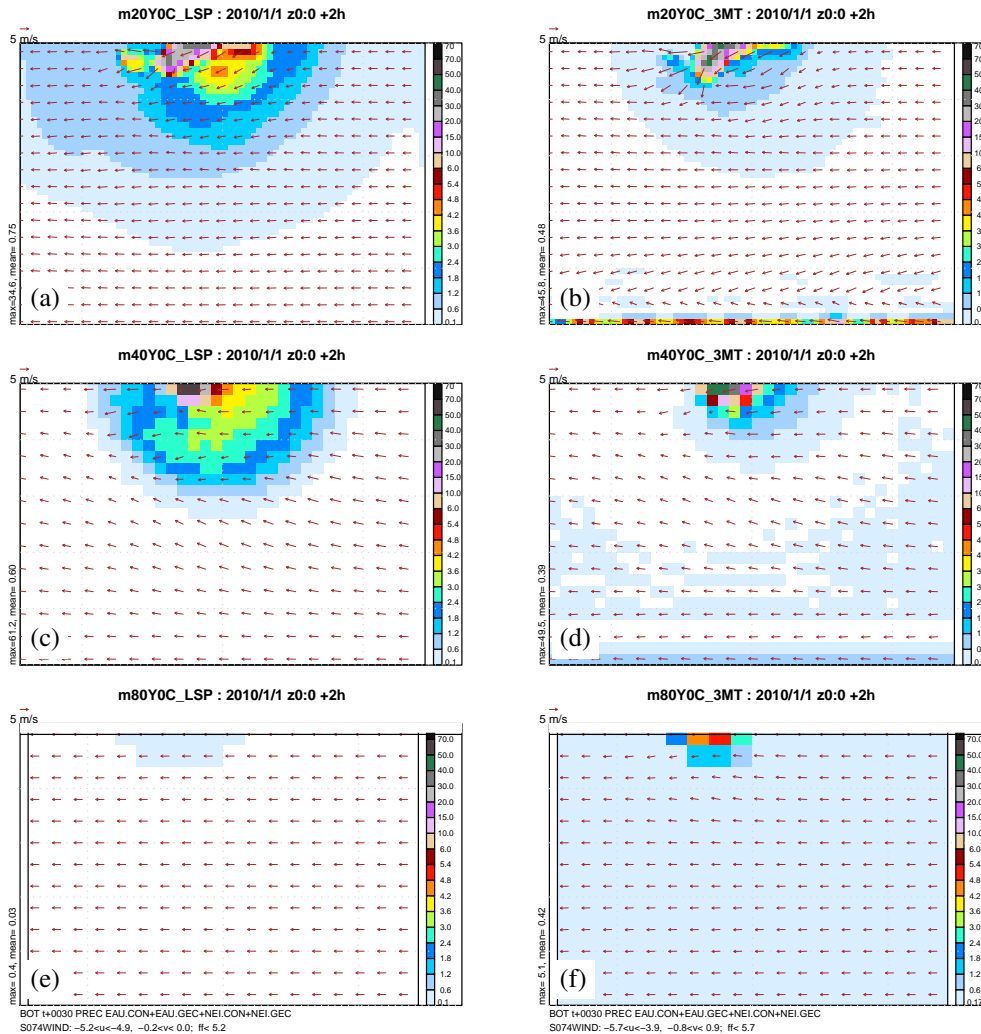


Figure 2: 2-hour accumulated parametrization, over the lower half of the symmetric domain. Left: ‘dia’; right: ‘3MT’ scheme. (a,b):  $\Delta x=2\text{km}$ ; (c,d):  $4\text{km}$ ; (e,f):  $8\text{km}$ .

length. For the academic experiment, we observe (Fig. 2, right column) that the forecast is still excessive at  $4\text{km}$ , and that the absence of an explicit triggering criterion allows an unwanted triggering (but with low precipitation) in an area around the main perturbation at the three resolutions.

In order to produce a gradual extinction of the subgrid scheme while increasing the resolution, we had to develop a scheme with a set of additional features.

Considering that with increasing resolution, the mean grid-box motion and resolved condensation represent an increasing fraction of the real subgrid updraught, the idea is that the subgrid scheme has to provide a decreasing contribution representing a complement to the resolved part. This *complementary subgrid updraught* (CSU) scheme keeps the 3MT sequential organisation, with a single call to the microphysical scheme, after combining subgrid and resolved condensation. The ascent properties are expressed as perturbations to the mean grid-box values, derived from the anelastic equations. The CSU-perturbation ascent is then closed and confined in a single model-column, and affected by the mesh fraction and the subgrid environmental profile. Evolution equations are used for the perturbation updraught velocity and the mesh fraction, and they allow (unlike in 3MT) the gradual rise of the updraught top along several time steps. The CAPE closure also requires special care, since the grid-column CAPE normally decreases with increasing mesh fraction (CAPE would be zero when the updraught covers the entire grid-column area, hence we cannot write that the mesh fraction is proportional to the grid-column

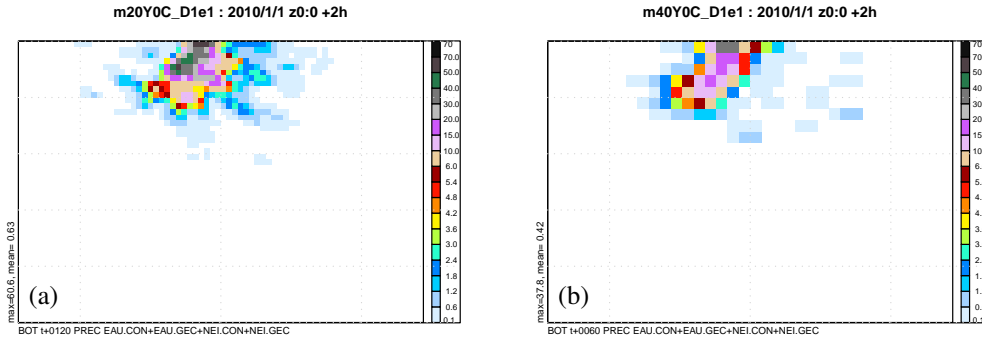


Figure 3: 2-hour accumulated surface precipitation, CSU scheme but using Kain 2004’s triggering criterion with fixed threshold,  $w_0=0.02\text{m/s}$ . (a):  $\Delta x=2\text{km}$ ; (b):  $4\text{km}$ .

CAPE). For this we try to evaluate the CAPE for an environment outside the updraughts. Finally a triggering criterion is introduced. Commonly used triggering criteria (e.g. Kain 2004, using a threshold of resolved vertical velocity  $\bar{w}$  but also energetic criteria like Rogers and Fritsch 1996, those based on CKE/TKE and CIN, or on moisture convergence) tend to produce more intense triggering with increasing resolution; and often an initial triggering has a positive feedback on further triggering in the neighbourhood, which can deteriorate the results in the vicinity of triggered ascents. In the present academic simulation, where CAPE is present over the entire domain, this phenomenon is critical. In the approach of Kain 2004, a mixed parcel is lifted up to its lifting condensation level (LCL) where it receives a buoyancy kick expressed by

$$\Delta T_{v,KF} = \left[ \gamma (\bar{w}_{LCL} - w_0 \min(1, \frac{z_{LCL}}{z_0})) \right]^{1/3}, \quad \frac{1}{\gamma} \sim 0.01 \text{m s}^{-1} \text{K}^{-3}, \quad z_0 = 2\text{km}, \quad w_0 = 0.02 \text{m s}^{-1}. \quad (1)$$

If the parcel is then able to reach its LFC and continue upwards, the scheme is triggered. In (1) the buoyancy kick increases together with the mean grid-box velocity  $\bar{w}$ , that should on its turn increase together with the updraught mesh fraction. Larger mesh fractions occur at higher resolution, but we can hardly find a general rule to increase the threshold  $w_0$  in function of the resolution, because the variation of the mesh fraction depends on the granularity of the updraughts in the mesh. Fig. 3 shows the total precipitation at 4km and 2km when using a fixed value of  $w_0$ .

We developed an alternative criterion consistent with the CSU-spirit, based on a threshold of resolved condensation, proportional to the inverse of the grid box area. This was used in the CSU experiment shown on Fig. 1 (right). In this case, the precipitation area appears consistent at the four resolutions, while the subgrid contribution is decreasing regularly with increasing resolution (not shown).

### 3 Real case

The model was tested with full physics at the same four resolutions on the thunderstorms of 2005-09-10 over Belgium. The runs are hydrostatic at 8 and 4km, and non-hydrostatic at 2 and 1km; there are 41 vertical hybrid levels. The *nocp* 1-km run is taken as a control, while the final reference is now the 1-hour accumulated radar image (Fig. 4).

Using the CSU scheme (Fig. 4 a,b,d,e), the structure of the precipitation is quite similar at the four resolutions, while the grid-box averaged amounts decrease at coarser resolution. The CSU manages to suppress the spurious band of intense precipitation at the Northern edge of the domain appearing on the control. The number of kernels at 1km is closer to reality and we observe a slightly better North-South alignment for CSU on the Western side, which corresponds to the location of subgrid activity as can be seen on Fig. 5.

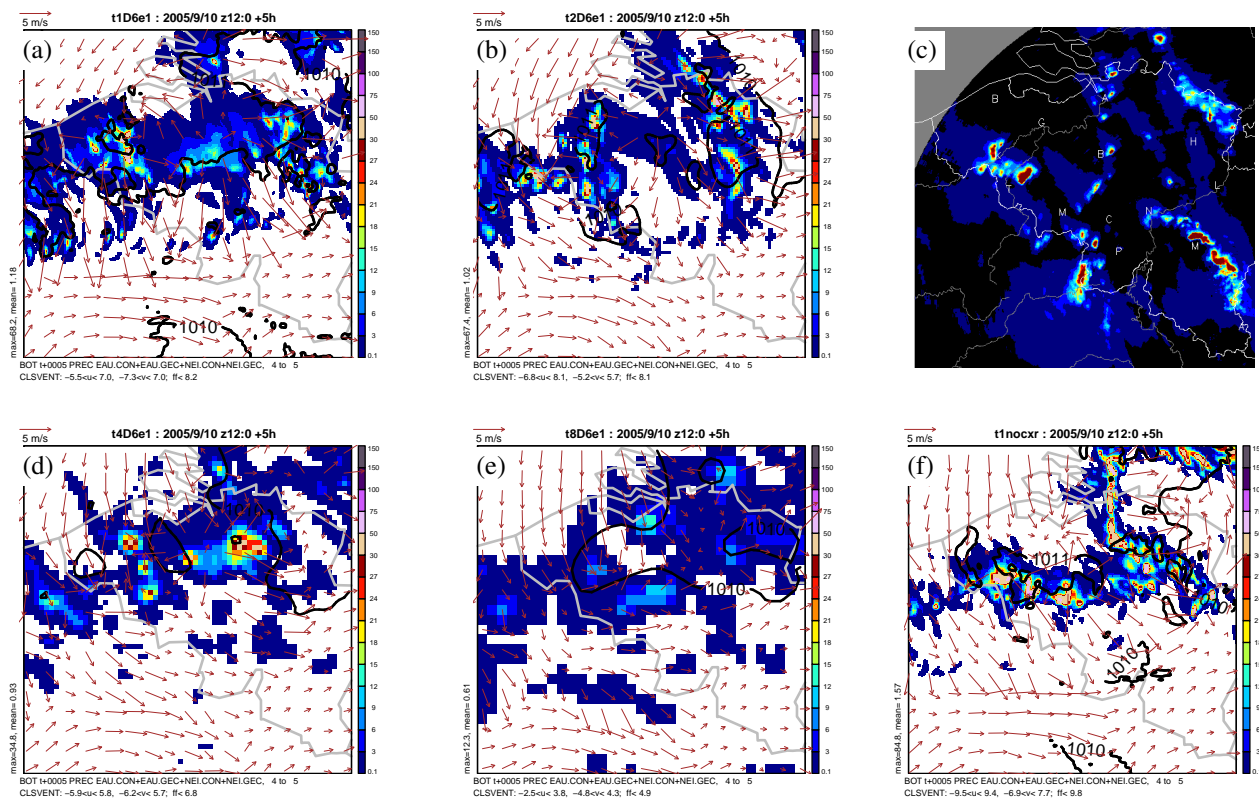


Figure 4: Thunderstorms of 2005-09-10 over Belgium. 10-m wind and 1-hour accumulated precipitation, forecast using the CSU scheme at 1km (a), 2km (b), 4km (d) and 8km (e) resolution. 1-hour accumulated radar image (c, same colour scale) and control simulation *nocp* at 1km resolution (f).

Fig. 7 shows the results at 2, 4 and 8km resolution with no DC parametrization (*nocp*), with a diagnostic parametrization (*dia*) and with *3MT*. At this particular range the *nocp* experiments does not show very intense ‘grey-zone syndrome’ at 4 and 2km, but this is not the case for the whole simulation. The unwanted band of intense precipitation is still present on the *nocp*-2km, and there is still excessive activity in this region at 4km. The amounts at 8km are clearly exaggerated. The diagnostic parametrization produces very large areas of intense precipitation at 4km and 2km, mostly due to the DC scheme. At 8km the amounts remain much too big when considering the averaging effect. The alignment and location with the diagnostic parametrization is quite similar to the one with no parametrization. Here the *3MT* response at 4km, while less extreme than the diagnostic scheme, is still excessive (the behaviour varies from one range to the next). The forecasters are generally happy to receive a warning even on a coarse resolution model grid, but this comes often together with an over-estimation of the precipitation that should represent an average over a large grid-box. In that case the results give no good estimation of the accumulation in hydrological basins.

Fig. 6 shows the accumulation over the entire area of Fig. 4. Unlike *nocp* and *3MT*, the CSU scheme appears to produce (at the end of the event) the same total amount of accumulated water at all four resolutions.

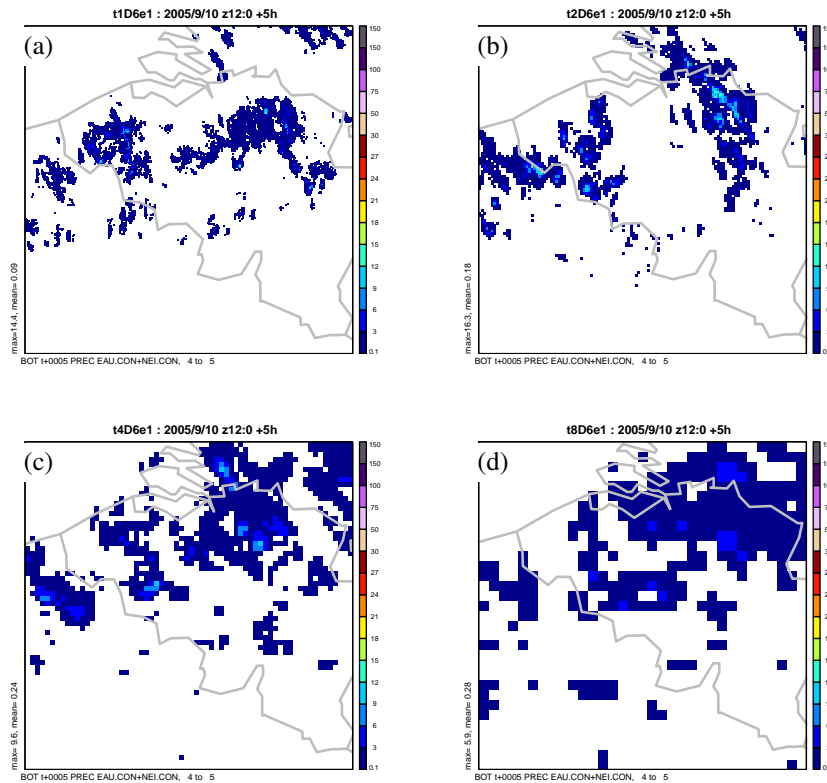


Figure 5: Same as Fig. 4 but subgrid share of the total precipitation, CSU scheme. 1km (a), 2km (b), 4km (c), 8km (d) resolution.

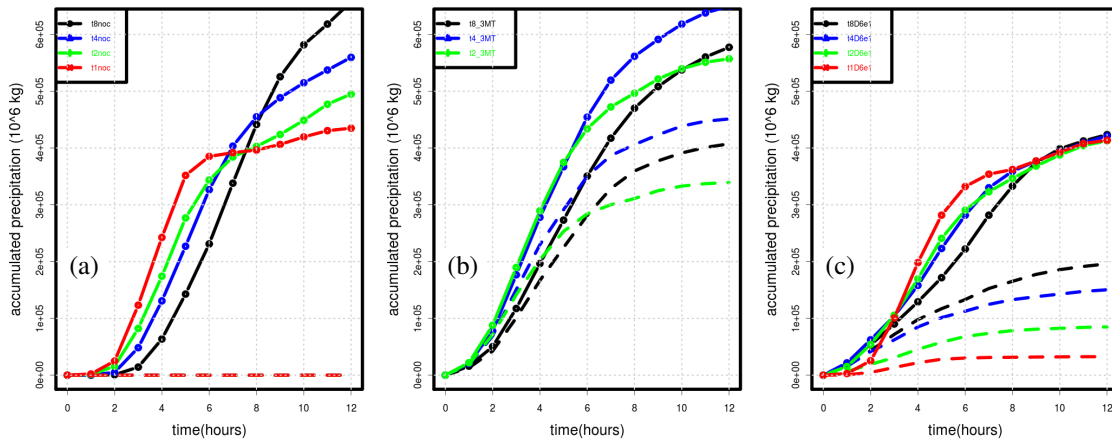


Figure 6: Evolution of accumulated surface precipitation. Red: 1km, green: 2km, blue: 4km, black: 8km. Solid line: total, dashed line: subgrid (DC-scheme) part. (a): ‘nocp’, (b): ‘3MT’, (c): ‘CSU’ simulations.

## 4 Conclusions

It appears possible to make consistent forecasts at the ‘grey-zone’ resolutions of the deep convection (between 8km and less than 1km, following the situation) by parametrizing aspects usually neglected at coarser resolution. The complementary subgrid updraught approach is specific for the triggering,

the representation of the ascent, the evolutive aspects, the closure, the organisation with the other parametrizations. Its features make it compatible with the full range of model resolutions, from several tens of km to less than 1km. It produces a gradual transition to fully resolved convection when the resolution becomes sufficient. The complementarity with the resolved scheme can allow to maintain the total amount of precipitation feeding the hydrological basins independently of the resolution, which is an asset for the coupling with hydrological simulations. Further tests are on the way to verify the good model behaviour when changing some other aspects of the physics and in a wider set of situations.

## Acknowledgements

This work benefited from enlightening exchanges in the frame of the COST ES0905 action subsidized by the European Community.

## References

- L. GERARD, J.-M. PIRIOU, R. BROŽKOVÁ, J.-F. GELEYN, and D. BANCIU. Cloud and precipitation parameterization in a meso-gamma scale operational weather prediction model. *Mon.Wea.Rev*, 137:3960–3977, November 2009.
- J. S. KAIN. The Kain-Fritsch convective parameterization: an update. *J. Appl. Meteor.*, 43:170–181, January 2004.
- Rogers, R. F. and J. M. Fritsch. A general framework for convective trigger functions. *Mon. Wea. Rev.*,124:2438–2452, 1996.
- M. L. Weisman and J. B. Klemp. The dependence of numerically simulated convective storms on vertical wind shear and buoyancy. *Mon.Wea.Rev*, 110:504–520, 1982.



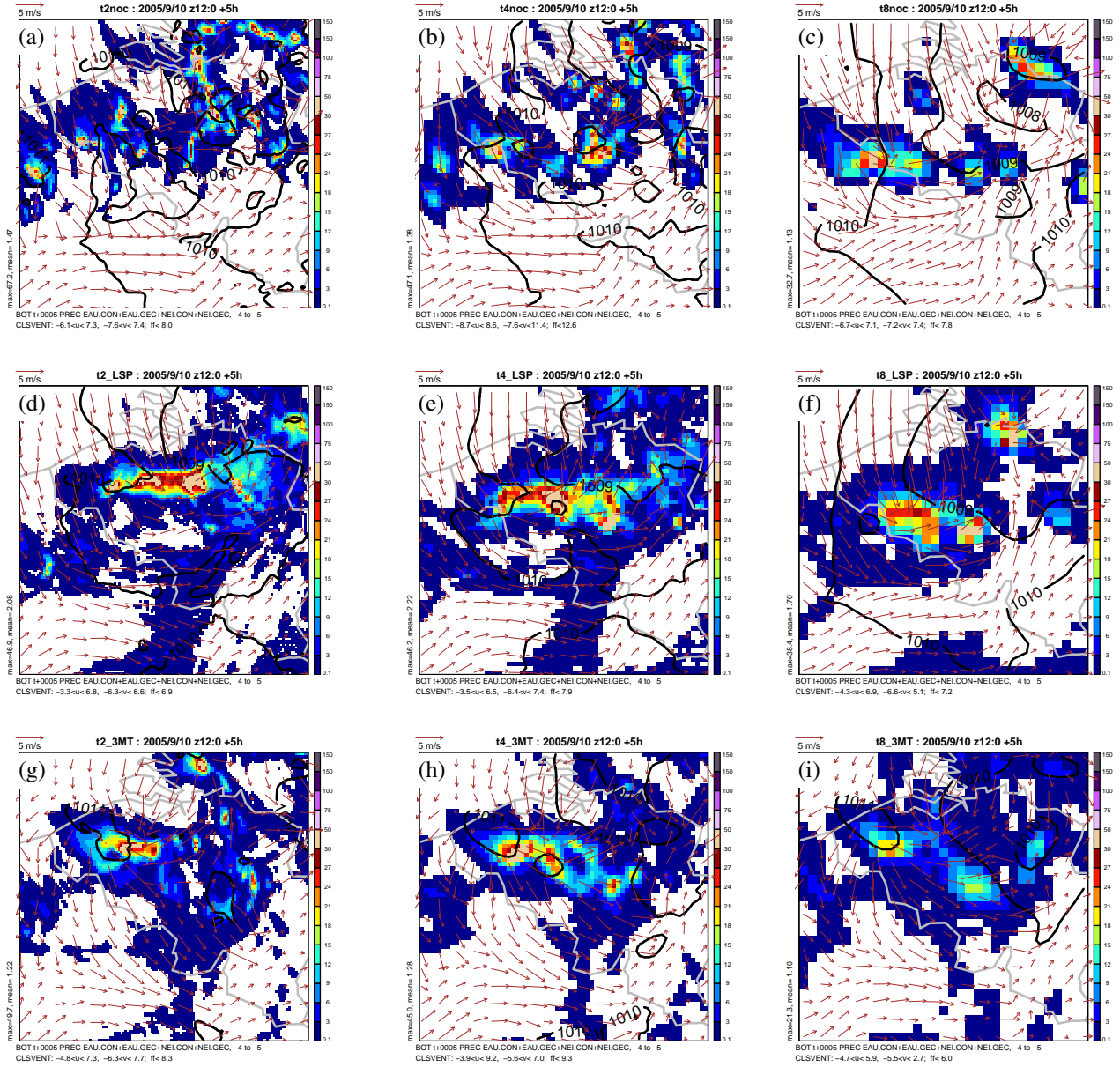


Figure 7: Same as Fig. 4 but for ‘nocp’ experiment at 2km (a), 4km (b), 8km (c), ‘dia’ experiment at 2km (d), 4km (e), 8km (f) and ‘3MT’ experiment at 2km (g), 4km (h), 8km (i) resolution.